

Evolution of the Nuclear Fuel Mechanical properties at high Burn-up An Extensive European Experimental Program

Daniel Baron*, Renaud Masson*, Jean-Marie Gatt*, José Spino**, Didier Laux***

* EDF R&D, CEA Cadarache, DEC/SESC, 13108 Saint-Paul-Lez-Durance cedex, France

** European Commission, Joint Research Centre, Institute for Transuranium Element,
PO Box 2340 Karlsruhe, D-76125 German

*** LAIN, Université Montpellier 2, 34095 Montpellier cedex 05, France

daniel.baron@edf.fr, phone : +33 6 87 31 99 37, fax : +33 4 42 25 29 49

Abstract

Computer codes have been developed in order to simulate the nuclear fuel rod mechanical behaviour, and therefore compare the evolution of the main parameters against a certain number of safety criteria, for reactor class 1 and class 2 operating conditions. Concerning the fuel material (UO_2 , MOX or UO_2 with additives) the mechanical properties have been determined on non irradiated samples. One can expect that these properties evolve with burn-up, due to the transmutation, the evolution of the oxygen potential, the accumulation of fission defects and in some case the material restructuring (High Burn-up Structure).

In order to provide the fuel thermo-mechanical calculation with more accurate mechanical properties, a large experimental project has been launched since several years by CEA, EDF and ITU ; furthermore a recent collaboration has been started with Studsvik, Sweden, concerning the possibility of performing in-pile creep measurements. The program is indeed organised in three folds, which can be described as follows:

1 - Acquisition of mechanical properties on non irradiated materials (UO_2 , UO_2+Gd , UO_2+Cr , MOX) with axial creep tests, three points bending tests up to 1700 °C, acoustic measurements at room temperature, instrumented micro-indentation tests and Vickers test from room temperature to 1200 °C. This allowed the development of a mechanical behaviour law available for these materials in the non-irradiated state.

2 - Acquisition of mechanical properties on irradiated materials in hot cells, using a micro-indentation machine developed especially in TUI, Vickers tests with the same machine, and a focused acoustic technique developed by the LAIN laboratory in the Montpellier University (France). The target is to define the evolution of the elastic properties, of the yield stress and of the thermal creep properties.

3 - More recently with the Studsvik Laboratories, the design of a specific rig for in-pile indentation has been completed. This aims at assessing the evolution of the irradiation creep properties, mainly in the HBS material.

Mechanical behaviour models are already achieved for non-irradiated materials and are presented. Concerning the acoustic methods, several presentations have already been published [2 to 7]. The main results are summarised. The micro indentation technique from room temperature to 1200°C is actually under qualification on non-irradiated samples. The state of the art is made. Finally an in-pile indentation concept is presented.

Keywords : Nuclear fuel, uranium dioxide, mechanical properties, acoustic, micro-indentation

INTRODUCTION

Computer codes have been developed in order to simulate the fuel rod mechanical behaviour, and therefore compare the evolution of the main parameters against a certain number of safety criteria. Improvement is still to be done in order to simulate the risk of cladding failure during an accidental power transient, due to the Pellet to Clad Mechanical Interaction (PCMI risk). PCMI results in the interaction between a cracked ceramic cylinder (UO₂ or MOX pellet) and metallic tubing (Zirconium cladding). The instantaneous strain on the cladding is mainly due to the differential thermal expansion between the fuel pellet and the cladding. Irradiated Zircaloy tubing is able to sustain an average deformation of 2 % without failure. Assuming no relaxation from the hot central part of the pellet (thermal creep) during the transient, the average pellet outward strain is never higher than 1.5 %. Therefore, one can expect that when a failure occurs, considerable local strains at pellet to clad interface are involved. The number of fuel radial cracks, and the fuel local properties at the pellet periphery are then certainly of first concern. Even if the risk of failure is demonstrated to be non-negligible at low burn-up (20-35 GWd/tM), this one appears to decrease with burn-up when, paradoxically, the potential amount of corrosive species increases.

One can conclude at this stage that the fuel pellet role in the PCMI simulation is of first order. Up to now, only non-irradiated fuel mechanical properties are provided for modelling. Compressive tests and three points bending tests have allowed developing thermal creep models. An additional term is provided from in pile experiments conducted in the seventies (reported in literature), in order to simulate the in-pile irradiation component. In these models, conceived up to 1000°C, the non-thermal irradiation component is dominant.

Observation reported several years ago on high burn-up pellets (60 GWd/tM) in standard PWR fuel have shown an axial fuel flow with a deformation of the chamfer (Figure 0.1). This let expect an increase of the irradiation activated creep in case of formation of the HBS (High Burn-up Structure) with a generalised grain subdivision and a drastic increase of the fuel porosity.

In order to provide the fuel thermo-mechanical calculation with more accurate mechanical properties, a large experimental project has been launched since several years by CEA, EDF and TUI [1]; more recently, discussions are engaged to make possible in-pile creep measurements. The general experimental scheme is given on Figure 0.2. The program is indeed organised in three steps, which can be described as follows:

1 - Acquisition of mechanical properties on non irradiated materials (UO₂, UO₂+Gd, UO₂+Cr, MOX) with axial creep tests, three points bending tests up to 1700 °C, acoustic at room temperature, micro-indentation tests and Vickers test from room temperature to 1200 °C. This has allowed the development of a mechanical behaviour law available for these materials in the non-irradiated state.

2 – Acquisition of mechanical properties on irradiated materials in hot cells, using a micro-indentation machine developed especially in TUI, Vickers tests with the same machine, and a focused acoustic technique developed by the LAIN laboratory in the Montpellier University (France). The target is to define the evolution of the elastic properties, of the yield stress and of the thermal creep properties.

3 – More recently with the Studsvik Laboratories, the design of a specific rig for in-pile indentation. This is aimed to assess an eventual evolution of the irradiation creep properties, mainly in the HBS material

Mechanical behaviour models are already achieved for non-irradiated materials and are presented. Concerning the acoustic methods, several presentations have already been published [2 to 7]. The main results are summarised. The micro indentation technique from room temperature to 1200°C is actually under qualification on non-irradiated samples. Details of the in-pile indentation device will be discussed at the end.

1 – VISCOPLASTIC MECHANICAL BEHAVIOUR MODEL DEVELOPED AT EDF-CEA FOR NON IRRADIATED UO₂

The viscoplastic behaviour of the nuclear fuel material depends upon several parameters as: grain size (d), porosity (p) and temperature (T). Both experimental (compressive tests) and theoretical approaches have been used to establish the constitutive Monnerie-Gatt law [9]. Accounting for the porosity influence, we have used, as Michel and Suquet did in ref [10], an elliptical potential which can be written:

$$\Psi = \frac{K(d, T)}{n+1} \left(\frac{9A(p)}{4} \sigma_m^2 + B(p) \sigma_{eq}^2 \right)^{\frac{n+1}{2}} \quad (1.1)$$

where n is a constant, K a function of the temperature and the average grain size; A and B are analytical functions of porosity. A is evaluated considering a porosity in the viscoplastic matrix. We have found :

$$A(p) = p(1 - p)^{\frac{-2n}{n+1}} \quad (1.2)$$

B is evaluated considering a modified secant method [11] linked to Mori-Tanaka model. We have found:

$$B(p) = \left(1 + \frac{2}{3}p\right)(1 - p)^{\frac{-2n}{n+1}} \quad (1.3)$$

In UO_2 , two time-dependent-strain mechanisms are observed [12], i.e., scattering-creep (associated to potential $\Psi_1 \sim 1/d^2$) and dislocation creep (associated to potential $\Psi_2 \sim (1 - \cos d/d_0)$). Therefore the final microscopic potential takes the form:

$$\Psi = (1 - \theta)\Psi_1 + \theta\Psi_2$$

with :
$$\theta = \frac{1}{2} \left(1 + \tanh \left(\frac{T - \omega \sigma_y^{-q}}{h} \right) \right) \quad (1.4)$$

ω , h , q being constant parameters and

$$\sigma_y = \sqrt{\frac{B_1}{B_1 + \frac{A_1}{4}} \sigma_{eq}^2 + \frac{9A_1}{4B_1 + A_1} \sigma_m^2} \quad (1.5)$$

For the scattering-creep, we take:
$$K(d, T) = \frac{K_1}{d^2} e^{\frac{-Q_1}{RT}}, \quad (1.6)$$

and for dislocation creep, we take:
$$K(d, T) = 2K_2 d_0^2 \left(1 - \cos \frac{d}{d_0}\right) e^{\frac{-Q_2}{RT}}, \quad (1.7)$$

with K_1 , K_2 , Q_1 and Q_2 constant parameters.

The total creep strain can then be written as:

$$\dot{\epsilon}_{vp} = (1 - \theta) \frac{\partial \Psi_1}{\partial \sigma} + \theta \frac{\partial \Psi_2}{\partial \sigma} + \frac{\partial \theta}{\partial \sigma} (\Psi_2 - \Psi_1) \quad (1.8)$$

The porosity evolution can be written as: $\dot{p} = (1 - p) \text{Tr}(\dot{\epsilon}_{vp})$

The constant parameters have been identified from compression creep tests data base (see Figure 1.1). The results of this identification are given in Table 1. The law has been validated on controlled strain rate tests. In Figure 1.2 one can see the good agreement between the theoretical and the experimental ultimate steady stress. Figure 1.3 shows finally a comparison between a three-points-bending test simulation and experimental data provided in the PhD work of Ref. [13]. The agreement is very satisfactory.

n_1	m_1	Q_1	K_1
1	-2	377 KJ/mol	$7.57 \cdot 10^{-14}$ (SI)
n_2	d_0	Q_2	K_2
8	15 μm	462 KJ/mol	$2.54 \cdot 10^{-44}$ (SI)

h	ω	q	
600 K	47350	0.189	

Table 1.1

2 – LOCAL ELASTIC CONSTANTS USING THE LAIN FOCUSED ACOUSTIC SIGNATURES METHOD.

Since 1996, the LAIN group (Laboratoire d'Analyse des Interfaces et de Nanophysique) of the University of Montpellier is working in tight collaboration with Electricité De France (EDF), the Commissariat à l'Energie Atomique (CEA) and the Institute for TransUranium Elements (ITU) for high burn-up fuel elastic properties assessment using local micro-acoustic methods. During these years several milestones have been achieved: a micro-acoustic device has been installed in hot cell at ITU in Karlsruhe, calibration laws have been established for local volume fraction of porosity in non irradiated UO_2 , the effect of grain size on elastic properties of non irradiated UO_2 as been quantified, and the impact of additives on elastic moduli has been evaluated. All these results have already been published in international journals or presented in congress [2-8]. More recently, the effect of stoichiometry and U_4O_9 - phase precipitates have been quantified and the global elastic parameters has been assessed on irradiated fuel (HBRP samples and N118 BR3 rod) from 0 to 100 GWd/tM. Such results, which at this date are unique, constitute an important progress for irradiated UO_2 behaviour understanding [14].

2.1 – Fundamentals of the acoustic methods

The theory of elasticity in an isotropic material such as sintered UO_2 shows that only two ultrasonic velocities are needed to assess the elastic constants [15-18]. Usually, longitudinal (V_L) and the transverse (V_T) velocities are measured [19]. For local measurements, frequencies between 50 and 200 MHz are needed. In this range, the transverse signal attenuation on irradiated fuel is so high that the transverse velocity is not measurable. Consequently, we have chosen to use another ultrasonic wave: the Rayleigh surface wave. Its velocity will be called V_R in this paper. With the knowledge of V_L and V_R , the transverse velocity V_T is deduced using the relations (2.1) and (2.2) [20].

$$V_T^8 - (V_L^2 + V_R^2)V_T^6 + \frac{3}{2}V_L^2V_R^2V_T^4 - \frac{1}{2}V_L^2V_R^4V_T^2 + \frac{1}{16}V_L^2V_R^6 = 0 \quad (2.1)$$

$$0 \leq V_T \leq \frac{V_L}{\sqrt{2}} \quad (2.2)$$

The elastic moduli (E and G) and the Poisson's ratio ν are then derived as follows [21]:

$$E = \rho V_T^2 \frac{3V_L^2 - 4V_T^2}{V_L^2 - V_T^2} \quad (2.3)$$

$$G = \rho V_T^2 \quad (2.4)$$

$$\nu = \frac{1 - 2\left(\frac{V_T}{V_L}\right)^2}{2\left(1 - \left(\frac{V_T}{V_L}\right)^2\right)} \quad (2.5)$$

where ρ is the density.

For measurements on nuclear fuel oxide, the Rayleigh surface wave velocity is obtained from acoustic signature [22-23] (Figures 2.1 and 2.2). However, in most cases, the wave attenuation is too high so as to detect the longitudinal velocity in the signature. Therefore, this last velocity is measured using an echography on fuel samples slices of about 1mm in thickness (Figure 2.3). Assuming a very low variation of the Poisson ratio around a value of 0.3, relations 2.3 and 2.4 can be simplified as follows [6]:

$$\nu = 0.3 \Rightarrow \begin{cases} E \approx 3\rho V_R^2 \\ G \approx 1.162\rho V_R^2 \end{cases} \quad (2.6)$$

2.2 – Acquired results

With the ultrasonic device presented here above, we can in principle directly assess in a local way to the elastic moduli on nuclear fuel cross-section samples prepared for ceramography. However, the analysis of the measured data is complex because they depend simultaneously on several parameters, like, e.g., precipitates, gaseous fission products, irradiation defects, stoichiometry evolution, grain size, etc. [24].

So, for the elastic moduli E or G we can write:

$$E = f(\text{porosity, FP precipitates, FP in solid solution, trapped gaseous FP in matrix, O/M ratio, point defects, etc}) \quad (2.12)$$

Since from the experimental point of view, performing measurements on each parameter separately is almost impossible, a number of simplifications and assumptions must be introduced in the above formulation, which can be resumed as follows:

- the effect of porosity and bubbles is the same (i.e., via cavity volume fraction) and is independent of the gas pressure inside the cavities.
- the irradiation defects have only an effect on attenuation and not on the velocities
- the effect of grains size has no effect on velocities [5]
- the effect of metallic FP and FP in solid solution can be evaluated with simulated fuels. This will give a global effect of burn-up.

Consequently, the relation (2.12) has been simplified as follows:

$$E = f(\text{porosity, O/M ratio, global Burn - up}) \quad (2.7)$$

Concerning the porosity effect, the EdF-CEA studies [2,8,14] on the application of the Berryman's model [25,26] led to the following relations:

$$\frac{E}{E_0} = 1 - (0.36 * \ln^2(w) + 2.000) * p \quad (2.8)$$

$$\frac{G}{G_0} = 1 - (0.28 * \ln^2(w) + 1.920) * p \quad (2.9)$$

where w is the pore shape factor for oblate pores. All Berryman's model, periodic homogenisation methods [6] and models based on minimum contact area [14], [27,28] lead to w -values in the range 0.25 for as fabricated pores, which are mainly of intergranular nature. A value of 1 for this variable is more adequate for the irradiation induced intragranular pores, as found in the rim region of high burn-up fuels. However, for this value of w , and for porosity levels > 0.1 , Eq. (2.8) leads to E/E_0 values quite below the expected range for the rim material as from hardness measurements [30]. A verification of this law for irradiated fuels, particularly at high burn-ups, appears therefore still necessary.

As for the effect of the oxygen stoichiometry (O/M) our experiments showed that it was negligible for UO_{2+x} , as far as U_4O_9 precipitates were not formed. Forlano [31] has indeed observed, as we did, a very important effect of the U_4O_9 precipitates on the elastic moduli. With this reserve, our results are satisfactorily consistent with the open literature [30-34]. However, for irradiated fuels this aspect appears not relevant because it has been shown that the oxygen potential in PWR-fuels under normal operating conditions stays relatively unchanged and near the value of the stoichiometric material (O/M=2). With this in mind, the main parameters affecting the E-values remain thus the porosity and the global burn-up.

Figure 2.5 shows the whole set of measurements obtained by this method, including simulated samples manufactured at ITU and in Chalk River (AECL) [35], two sets of irradiated UO_2 and $UO_2+5\%Gd$ samples from the High Burn-up Rim Project with irradiation temperatures ranging from 500 to 1200 °C and burn-ups ranging from 35 GWd/tM to 100 GWd/tM [36,37], and a N118 BR3 fuel sample with an average pellet burn up of 68 GWd/tM [38]. For all measurements presented in Fig. 2.5 the Young modulus has been deduced from the V_R value using relation (2.6) and plotted against the burn-up. For the shear modulus, which is not reported here, a global trend similar to that of the Young's modulus was found.

Despite scatter of the results, the whole data show a general decrease of the elastic modulus with burn-up (pure UO_2 taken as reference), particularly in the burn-up range 0-50GWd/tM where for irradiated fuels still no high burn-up transformation has occurred (Figure 2.5). Correction of these results by porosity according to (2.8) does not change the general trend observed. However, these data, as such, are in contradiction with the widely accepted trend showing the elastic modulus of a material to be directly proportional to its hardness [39-42]. The hardness of the irradiated fuels has been unambiguously proven to increase up to 50 % in the burn-up range 0-70 GWd/tM [29].

Because of the appeared controversy, which for the moment can not be clarified, a series of alternative measurements of the elastic constants of UO_2 and doped UO_2 by other techniques than the acoustic method has been undertaken at ITU [43], the results of which are summarized in the next section.

3 – ELASTIC MODULUS VIA SYNCHROTRON DIFFRACTION UNDER PRESSURE (LATTICE COMPRESSIBILITY) AND KNOOP INDENTATION METHODS.

In another work conducted at ITU by Pujol et al [43], the elastic constants of pure UO_2 and simulated spent UO_2 fuels were determined using synchrotron powder diffraction under pressure and Knoop indentation techniques. The first technique provides the bulk modulus of the material, or compressibility of the lattice, B_0 , by monitoring the shift of the Bragg's reflections positions during pressure application. From the B_0 value the E-modulus is calculated on assuming a value for the Poisson's ratio (in this case taken as 0.32 for pure UO_2 [32] and 0.31 for doped UO_2 [44]) [43]. The second technique, i.e., Knoop indentation, provides the proportionality constant between the hardness and the elastic modulus, i.e. the H/E ratio, which is determined from the contraction of the diagonals of a strongly asymmetric indentation [52, 53]. Using the determined H/E ratio, the value of E is then obtained from the H-value measured separately by Vickers indentation [41,42,43].

Figure 3.1 summarizes the results obtained by both techniques as a function of burn-up. The E-values from the synchrotron measurements are plotted on the left hand y-axis. The E-values derived from the Knoop indentation method are plotted on the right hand y-axis. Consistently with the previously mentioned premise of the elastic modulus being proportional to the hardness of a material, both plots in Fig. 3.1 show an increase of the E-modulus of UO_2 on increasing the (simulated) burn-up, i.e. on increasing the amount of FP in the fuel matrix.

Both methods in this section provide information of the elastic properties in the atomic and microscopic scales, i.e., on what can be called the intrinsic elastic behaviour of the material. Differently, the method of the former section provides information of the elastic properties of the material but in a macroscopic scale where also heterogeneities like porosity, cracks, second phase precipitates, etc., play an important role. Thus, as partially mentioned in [43], an influence of the microstructure to explain the discrepancies of the methods is very likely.

4 – INDENTATION TESTS FROM ROOM TEMPERATURE TO 1200°C

4.1 - Instrumented indentation device

Following a large series of Vickers indentation tests on irradiated fuels at room temperature whose main results have been already published [45], an instrumented indentation device targeted to operate in Hot Cells up to temperatures of 1200 °C has been designed and constructed at ITU, and is now being validated with non-irradiated samples.

The aim of the installation is to perform indentation tests on pre-selected regions of polished fuel cross-sections by monitoring simultaneously the applied load and the penetration depth as a function of time. With the selected configuration simple load tests, creep tests and stress relaxation tests are possible. Apart from the construction difficulties implied by the necessity of operating the apparatus in Hot Cells, crucial problems to solve were the temperature drifts and the sensing of the real penetration depth, which is usually spoiled by the creep down of the sample support table. The last made necessary the development of special calibration procedures to determine the equipment compliance as a function of temperature.

Examples of room temperature measurements with the apparatus are given in Figures 4.1 and 4.2. Figure 4.1 shows determinations of the E-modulus of SS 316L and porous glass samples, the first assessed with 5 % accuracy respect to the tabulated standard value [46]. Figure 4.2 shows data of an indentation-creep test on a SS 316L sample where the primary and secondary creep stages are clearly separated. The last figure puts also in manifest the high sensitivity of the device to determine penetration-depths changes in the submicron range. A similar quality of the measurements is expected to be achieved in the tests with the unirradiated and irradiated fuel samples.

4.2 – Finite Element Numerical Indenter

From the empirical analysis of the instrumented indentation tests results it is possible to obtain with good accuracy the E-modulus of the material, its universal hardness, H, and with some care, the constant deformation speed associated with the secondary creep stage, as a function of temperature. However, other parameters needed for the complete mechanical characterization of the material can only be obtained if a reliable mathematical description of the indentation field is available. With this mathematical framework the desired parameters can be extracted by the so-called inverse identification method, provided that a constitutive mechanical equation for the material is previously defined and validated. These two challenging tasks have been undertaken by EDF-CEA. Aspects of the developed constitutive equation were treated in section 1. This section deals with the 3D numerical indenter developed at EDF in the context of a PhD work done in collaboration with the Ecole Polytechnique, Paris.

The indenter is approximated by a conical shape to reduce the problem to a bi-dimensional (axi-symmetrical) one (see Ref. [10]). The corresponding two-dimensional mesh is optimized to save computing times (see Figure 4.3). Linear elements with axisymmetric conditions are adopted: eight microns square elements are used at the contact zone with indenter (the mesh has about 500 nodes).

Regarding the axi-symmetry of the geometry, a nil horizontal displacement is imposed along the axis of revolution. A similar condition is imposed to the right limit of the mesh while its bottom is fixed vertically. Lagrange's multipliers handle contact conditions.

The constitutive law presented in section 1 was recently introduced in the Finite Element Code Aster (<http://www.code-aster.org>). An implicit integration was adopted as follow: denoting by ε the total strain at time $t + \Delta t$ and $\Delta\varepsilon$ its variation during the time step, the unknowns are the variations of the stress, porosity and viscoplastic strain, respectively. These unknowns are solutions of a large system of non linear equations (7 scalar unknowns for axi-symmetric calculations), which can be reduced to the following two coupled non linear equations:

$$\begin{cases} 3 \mu \Delta t \frac{\partial \Psi}{\partial \sigma_{eq}} \left(\sigma_{eq}, \sigma_m^- + 3K \left(Tr(\Delta\varepsilon) - \frac{\Delta f}{1-f} \right), f, T \right) + \sigma_{eq} - \sigma_{eq}^e = 0 \\ \Delta f - (1-f) \frac{\partial \Psi}{\partial \sigma_m} \left(\sigma_{eq}, \sigma_m^- + 3K \left(Tr(\Delta\varepsilon) - \frac{\Delta f}{1-f} \right), f, T \right) = 0 \end{cases} \quad (4.1)$$

$\Delta f, \sigma_{eq}$ being the reduced unknowns. This reduction makes the implicit resolution easier and more robust.

Finite strains of the UO₂ sample are described with the help of the large displacement assumption. Concerning the indenter's mechanical behaviour, a rigid elastic constitutive law is adopted.

4.3 – First numerical results

At 1200°C, a 100 % dense UO₂ sample (grain size ≈ 6 microns) is indented up to 30 microns depth (constant 30 microns/h displacement rate), and then unloaded. The simulated displacement–load curve is reported on Figure 4.4 (continuous line). We have reported on the same Figure two alternative versions of the constitutive law presented in section 1. These two versions correspond to a theta-function equal to 0 (dotted line) or 1 (long dashed), which corresponds to low or high creep-stress regimes, respectively. Actually, high values of the stresses in the plastic zone are experienced during indentation. As a result, the theta-function is close to 1 in this region. That is the reason why, the second choice is very close to the original version of the constitutive law.

5 – PROJECT FOR AN IN PILE INDENTATION CREEP MEASUREMENT

5.1 – Description of the device

The creep component of the fuel material that is activated by irradiation at low temperatures is likely being underestimated with rising burn-ups. It means that the fuel pellets could less stress the cladding than assumed thanks to a better strain distribution at the interface. That is why EDF and its partners agreed on the necessity to conceive an experimental device, which could be operational under irradiation to characterise this creep component.

A first design of this device was recently issued (Figure 5.1). The principle of the device is based on the differential thermal expansion between the indenter and the capsule containing the irradiated fuel sample. In order to limit the fuel thermal gradient, the sample (wafer) is sandwiched between two molybdenum pellets. The fuel temperature is set to stay low enough (400 to 700 °C) to avoid any thermally activated deformation.

The indenter is sliding through a channel in the upper molybdenum pellet. At room temperature, the indenter stands on the shoulder of the capsule (Figure 5.1), which is made in Zircaloy-4 (Zy 4), like the cladding. This shoulder serves to avoid any contact between the indenter and UO₂ during shipment or during introduction in the irradiation location. Actually, any fretting before irradiation would falsify the imprint.

The material used for the indenter must have a thermal expansion coefficient twice higher than the Zy4 material used for the capsule. Stainless steel is proposed for the indenter line. This differential thermal expansion, when the temperature rises, allows establishing a contact between the indenter and the sample, pushing up the line and therefore applying the calibrated spring-load on the fuel wafer. A priori, 1 or 2 N are acceptable load-levels regarding mechanical tests performed out of pile, while the indenter radius can be first estimated around 1 mm. The heat is produced by the fuel wafer submitted to irradiation in the reactor and also by the gamma deposit coming from the core surrounding.

This configuration helps to generate imprints on the fuel material. Imprints will be characterised after different irradiation times to evaluate the rough evolution of the irradiation creep component for a standard set of input parameters, and the order of the thermal gradients in the fuel material as well.

The filling gas must be adjusted so that the range of temperatures desired can be reached. A priori, non-pressurized Helium (He) can be chosen for modelling. Argon (Ar) could be added to make the gas more thermally isolating. Taking into account the out of pile hardness tests performed in ITU, one must account for a large scatter of the indentation sizes, so that about 10 indentations for each material and each test- duration must be planned. This imposes the concept to be defined the simplest possible in order to perform a large number of tests as needed.

Modelling foresees a linear behaviour of the creep rate with the fission density. Therefore, in order to obtain measurable imprints in the shortest times, fission densities must be targeted the highest, as allowed by the remaining fuel activity.

5.2 – Device dimensioning [47]

Thermal dimensioning of the device has been conducted in order to optimise the design of the device. Calculations have been performed with the Finite Element Software Code Aster (free download at www.code-aster.org). A two-dimensional mesh has been set associated to a commands program both allowing working with variable parameters (figure 5.2). Calculations have been conducted accounting for the gamma heating or not. Figure 5.3, showing the temperature fields, demonstrates the benefit of the gamma heating to elevate the temperature of the indenter and then allow its elongation.

Temperatures calculated at the indentation location in the reactor are between 400 to 500 °C. This temperature range is representative of the fuel rim area.

Low temperature dependence has been observed on irradiation creep of fresh fuel. However, many observations and characterisations of high burn-up fuel let expect the presence of secondary phases on grain boundaries, which may be able to change the creep properties at low temperatures. In particular, Caesium Uranates studied ten years ago in Berton's PhD-work [48], were demonstrated to have a high creep propensity above a temperature threshold not far from 400°C. Obviously, the compounds formed at higher burn-up are certainly more complex than those simplified studied in [48] and temperature threshold could be different. Albeit, a certain temperature activation of irradiation creep due to the effect these kinds of 'soft' grain boundary phases potentially formed at high burn-ups is at all possible.

Calculations have been performed under the following conditions: 500W/cm Linear heat rating, 5W/g gamma heating, external temperature equals to 40°C and pellet's Burn up equals to 65 MWd/kgU. Starting from these data, the following modifications have been introduced: Argon have been preferred to Helium as filling gas while indenter's length is 10 cm. With this design, the proposed device has been proved to be realistic from a theoretical point of view.

Figure 5.4 illustrates the radial temperature distribution induced by the hole in the upper Mo-pellet for different axial positions in the fuel pellet. A hot area in the central upper part of the fuel appears clearly on this figure. The corresponding radial temperature difference reaches 121°C.

These theoretical results remain very sensitive to gamma-heating as well as solid-solid heat transfer (interstitial layer between the rod-Mo slices). To confirm these theoretical results, experiments on an instrumented mock-up are now needed. Further works are in progress including mechanical calculations so as to evaluate the in pile indentation time necessary to have a measurable imprint. However, especially for high burn-up materials, this needs for results of high-temperature indentations in order to fit properly the mechanical behaviour laws used for the calculations. These data is in preparation.

6 - CONCLUSIONS

Nuclear fuel material properties evolution with burn-up is needed to improve the computer code thermo-mechanical analysis, both for normal operating and accidental transient conditions. Although sensible progress has been made in the last twenty years in what concerns to thermal properties thanks to new laser flash techniques developed by UKAEA and then by ITU, the evolution of the fuel mechanical properties is still a problem that remains to be solved. Difficulties of this measurements are the sharp radial gradient of the properties and the pellet cracking pattern that make standard compressive or bending tests not applicable, particularly at high burn-ups. Recording this lack, a wide program has been launched since 1996 between EDF-CEA and ITU to provide new experimental data via local indentation measurements on irradiated fuel material, including the corresponding mechanical behaviour laws. The state of the art of this program has been described in this paper.

Thermal creep can be now assessed on irradiated samples, combining an indentation technique from room temperature to 1200 °C with a 3D numerical indenter used to fit the parameters of the law in order to reproduce the imprint shape, the load curve, the relaxation curve, or the creep curve. After a large number of technical difficulties now solved, the technique is already operative.

An alternative acoustic device has been developed in the same period to assess to the elastic properties evolution. Data has been acquired on many irradiated samples showing a decreasing trend and then a stabilisation. However, results of this technique disagree at this stage with alternative measurements of the elastic properties of UO₂ and doped UO₂ conducted at ITU by synchrotron powder diffraction under pressure and Knoop indentation techniques. Influence of the microstructure is a priori attributed to explain the discrepancies. The controversial results are expected to be definitely clarified on application of the instrumented indentation technique.

Concerning the fission induced component of creep, a simple device has been designed to perform in-pile indentation tests. These data are foreseen to complement thermal creep data to be obtained out of pile by high-temperature-indentation of irradiated fuel samples.

ACKNOWLEDGEMENTS

We are grateful to Ph. De-Bonnières (EDF/R&D) for his valuable help for the viscoplastic constitutive law's numerical integration in the Finite Element Code_Aster, and to Gunnar Lysell and his Studsvik team for the works enabling the design of a viable in pile indentation device.

REFERENCES

- [1] D. Baron, S. Leclercq, J. Spino, S. Taheri, "Development of a Micro-indentation Technique to determining the Fuel Mechanical Behaviour at high Burn-up", IAEA Technical Committee Meeting on Advances in Pellet Technology for improved Performance and High Burnup - Toranomon Pastral, TOKYO, JAPAN, 26 October - 1 November 1996
- [2] V.Roque, B.Cros, D.Baron, P.Dehaut, J. Nucl. Mater. 277 (2000) 211-216
- [3] V. Roque, D. Baron, J. Bourgoïn, J.M. Saurel, J. Nucl. Mater. 275 (1999) 305-311
- [4] D.Laux, G.Despaux, D.Baron, J.Spino, Proceedings of the 7th international conference on CANDU fuel, 23-27 Septembre 2001, Kingston, Ontario, Canada. Vol 1 and 2.
- [5] D.Laux, B.Cros, G.Despaux, D.Baron, J.Nucl Mater. 300 (2002) 192-197.
- [6] D.Laux, G.Despaux, D.Baron. Proceedings of the conference "Matériaux 2002". 21-25 October. Tours. France.
- [7] J.M. Gatt, Y.Monerie, D.Laux, D.Baron. Elastic behaviour of porous ceramics, published in J. Nucl. Mater
- [8] ITU activity report 2001. (EUR- 20252). Highlights 2001. Innovative Acoustic measurements of Elastic Modulus on Irradiated LWR-Fuels.
- [9] Y. Monerie, JM Gatt, *Overall viscoplastic behavior of non irradiated porous nuclear ceramics*, Mechanics of materials, 2005 Submitted.

- [10] JC Michel, P. Suquet, *The constitutive law of nonlinear viscous and porous materials*, J. Mech. Phys Solids Vol 40 N°4 pp 783-812, 1992
- [11] M. Bornert, P. Suquet, *Propriétés non linéaires des composites : approches par les potentiels*, in, *Homogénéisation en mécanique des matériaux*, M. Bornert, T. Bretheau, P. Gilormini, tome 2 Hermes science, 2001
- [12] P. Bohaboy, R. Asamoto, A. Conti, *Compressive creep characteristics of stoichiometric uranium dioxide*, GEAP-10054, General Electric Compagny, Sunnyvale, 1969
- [13] C. Colin, *Etude du fluage du dioxyde d'uranium: caractérisation par essais de flexion et modélisation mécanique*, Thèse de L'école Nationale Supérieure des Mines de Paris, 2003.
- [14] D.Laux. "Caractérisation mécanique de combustibles nucléaires à fort taux de combustion par méthodes micro-acoustiques." PhD thesis presented in University Montpellier II. 18 October 2002.
- [15] Gordon S.Kino. "Acoustic waves." Prentice-Hall, Inc. Englewood Cliffs, New Jersey 07632.
- [16] Daniel Royer, Eugène Dieulesaint. "Ondes élastiques dans les solides. Tome 1. Propagation libre et guidée." Enseignement de la Physique. Masson 1996.
- [17] Jérôme Sirven. "Les ondes : du linéaire au non linéaire." Masson Sciences. Dunod 2000.
- [18] Rohn Truell, Charles Elbaum, Bruce B.Chick. "Ultrasonic Methods in Solid State Physics." Academic Press. New York and London. 1969.
- [19] C. H. Schilling. J. N. Gray. "Non destructive Evaluation of Ceramics." Ceramic Transactions. Volume 89. Published by The American Ceramic Society. Westerville, Ohio.
- [20] I.A. Viktorov, "Rayleigh and Lamb waves", Plenum, New York (1967).
- [21] B.A Auld, Acoustic fields and waves in solids. Vol.I. A Wiley-Interscience Publication.
- [22] Briggs G.A.D., Acoustic Microscopy, Oxford : Clarendon press, 1992
- [23] D.Laux, G.Despaux, F.Augereau. "Improvement of the minimal characterisation size available by acoustic microscopy for mechanical parameters evaluation". European Physical Journal. Applied Physics. Vol. 17. 2002.
- [24] Donald R.Olander. "Fundamental Aspects of Nuclear Reactor Fuel Elements." 1976.
- [25] James G.Berryman. "Long-wavelength propagation in composite elastic media I. Spherical inclusions." J.Acoust.Soc.Am 68(6), Dec 1980. pp 1809-1819.
- [26] James G.Berryman. "Long-wavelength propagation in composite elastic media II. Ellipsoidal inclusions." J. Acoust. Soc. Am 68(6), Dec 1980. pp 1820-1831.
- [27] A.K. Mukhopadhyay, K.K Phani. "Young's modulus-porosity relations : an analysis based on a minimum contact area model." Journal of materials science 33(1998) 69-72.
- [28] A.K. Mukhopadhyay, K.K Phani. "An analysis of microstructural parameters in the minimum contact area model for ultrasonic velocity-porosity relations." Journal of the European Ceramic Society 20 (2000) 29-38.
- [29] J. Spino, J. Cobos-Sabate and F. Rousseau, "Room-temperature microindentation behaviour of LWR-fuels, part 1: fuel microhardness". J. Nucl. Mater. 322 (2003) 204-216
- [30] Roberto Forlano, A.W.Allen, R.J.Beals. "Elasticity and anelasticity of uranium oxides at room temperature: I, Stoichiometric Oxide. II, Hyperstoichiometric oxides. Journal of the american Ceramic Society. Vol 50-N°2-93-96. Vol 51-N°4-192-195.
- [31] N.Igata, K.Domoto. "Fracture stress and elastic modulus of uranium dioxide including excess oxygen." Journal of nuclear materials 45 (1972/73) 317-322
- [32] D.G.Martin. "The elastic constants of polycrystalline UO₂ and (U,Pu) mixed oxides : a review and recommendations. High temperatures-High pressures, 1989, volume 21, pages 13-24.
- [33] A.Padel, Ch. De Novion. "Constantes élastiques des carbures, nitrures et oxydes d'uranium et de plutonium." Journal of nuclear materials. 33 (1969) 40-51.
- [34] R.Scott, A.R.Hall, J.Williams. Journal of nuclear materials. 1 (1959) 39-48
- [35] P.G.Lucuta, R.A.Verrall, Hj.Matzke, B.J.Balmer, "Microstructural features of SIMFUEL-Simulated high-burnup UO₂-based nuclear fuel", Journal of Nuclear Materials 178, 48-60 (1991).
- [36] Hj.Matzke, V. Meyritz, K. Richter, C.Fuchs. Technical report. HBRP report 1. Fabrication of fuel discs for the IFA-601-Irradiation (1994). ITU Karlsruhe.
- [37] M.Kinoshita - CRIEPI – "Final report of High Burnup Rim Project (HBRP)", 16 February, 2001. Report Nr HBRP 5. European Commission. Directorate-General JRC. Joint Research Centre. Institute for Transuranium Elements (Karlsruhe site). Material research., Confidential. Karlsruhe, November 17, 2000.
- [38] Technical report. Institute for TU Elements. Joint Research Centre European Commission. "Post irradiation examination of fuel rods BR3-N118." Contract: T20L14/7B2711/RNE456 between Euratom and EDF.
- [39] D. Tabor, The Hardness of Metals, Clarendon, Oxford, 1951
- [40] R.W. Rice, Porosity of ceramics, Marcel Dekker, 1998.
- [41] D. B. Marshall, T. Noma, A.G. Evans, J. Am. Ceram. Soc. 65 (1982) C 175.
- [42] B.R. Lawn, V. R. Howes, J. Mater. Sci. 16 (1981) 2745.

- [43] M.C Pujol, M.Idiri, L.Havela, S. Heathman, J.Spino, "Bulk and Young's Modulus of doped UO₂ by Synchrotron Diffraction under High Pressure and Knoop Indentation", JNM 324 (2004) 189-197
- [44] M.O. Marlowe, A. K. Kaznoff, in: Ceramic Nuclear Fuels, Int. Symp., 3-8 May 1969, Washington, DC, The American Ceramic Society, Ohio, USA, 1969
- [45] N. Tardieu, A. Constantinescu "On the determination of elastic coefficients from indentation experiments". Inverse Problems, Vol. 16, (2000), p. 577-588
- [46] A. Bocaccini, J. Spino, Annual Amer. Cer. Soc. Meeting, Cocoa Beach, 2001.
- [47] R. Masson, V. Hure, D. Baron "Design's calculations of an in pile indenter device Document interne EDF. HT-25/04/030/A2005, January, 2004.
- [48] J-P Berton, D. Baron, M.Coquerelle, "Chemical stability and physical properties of Caesium Uranates", IAEA Technical Committee Meeting on Advances in Pellet Technology for improved Performance and High Burnup - Toranomon Pastral, TOKYO, JAPAN, 26 October - 1 November 1996

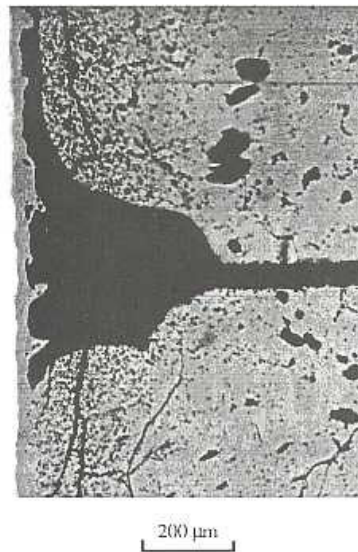


Figure 0.1 – evidence of a rim axial creep

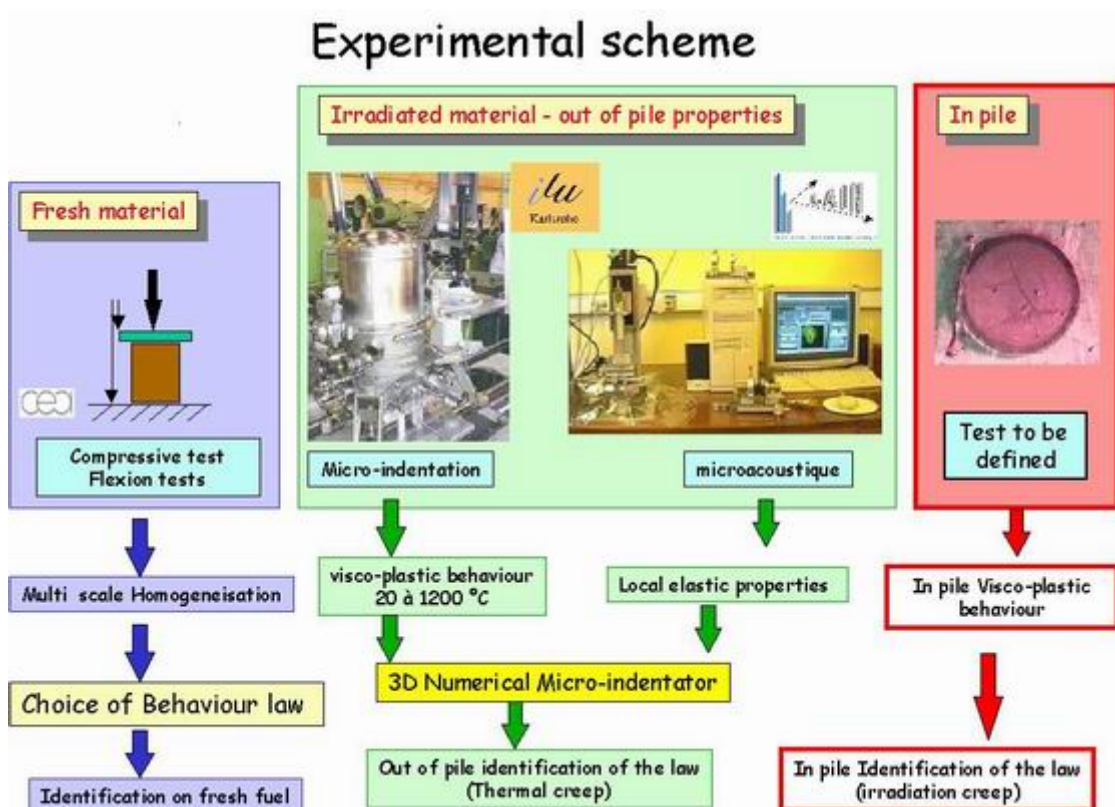


Figure 0.2 – Experimental scheme to assess to the evolution of the fuel mechanical properties with burn-up

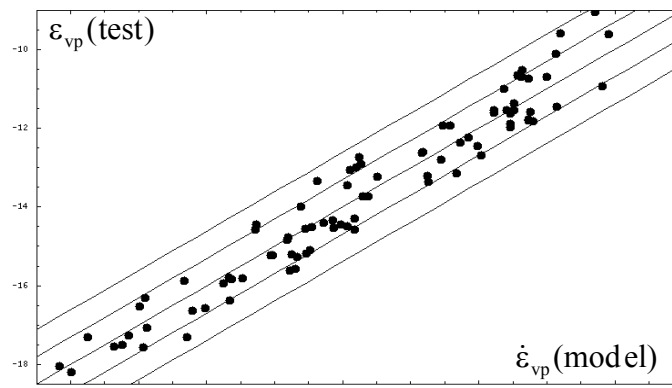


Figure 1.1 : uniaxial strain rate : comparison between numerical simulations and experimental data.

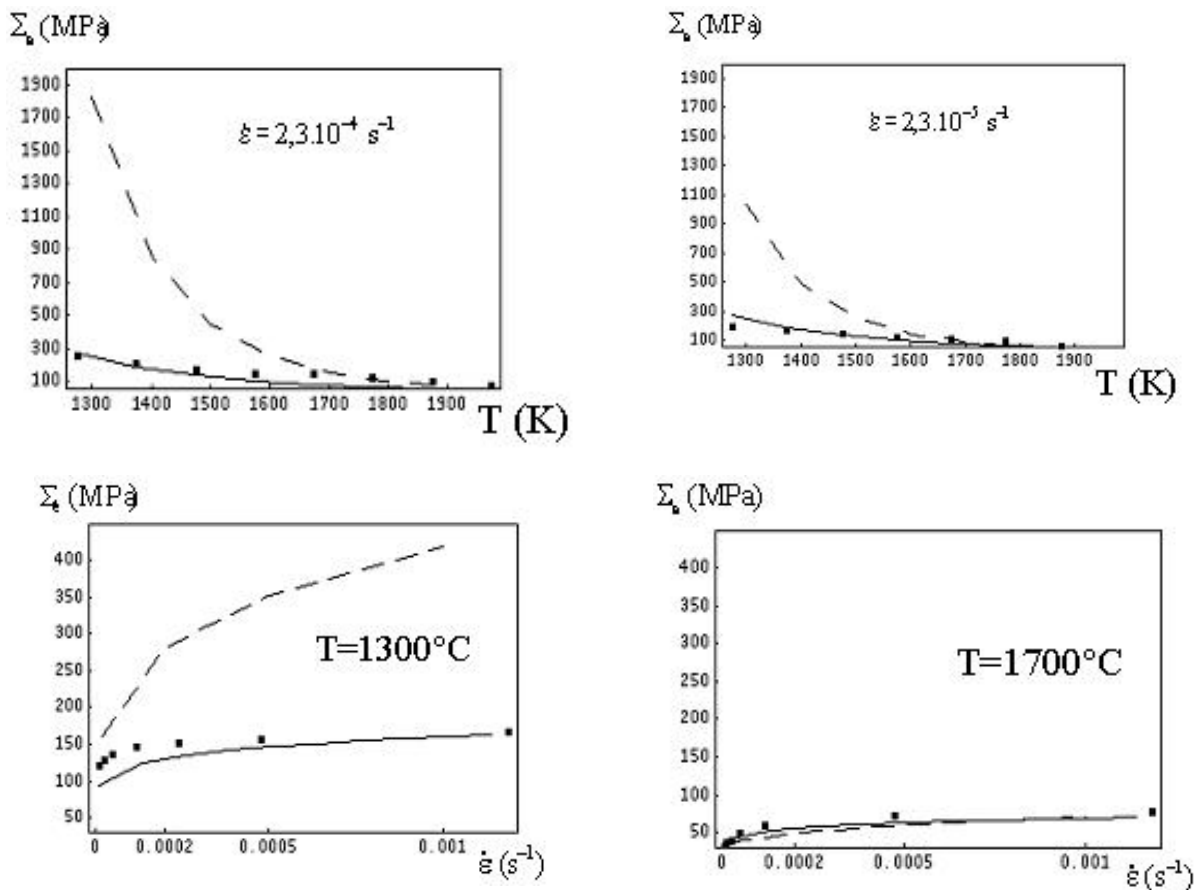


Figure 1.2 : Comparison between experimental (Square) and theoretical (present model : continuous curve, former model : dashed curve) ultimate steady stress at different temperature and different controlled strain rate.

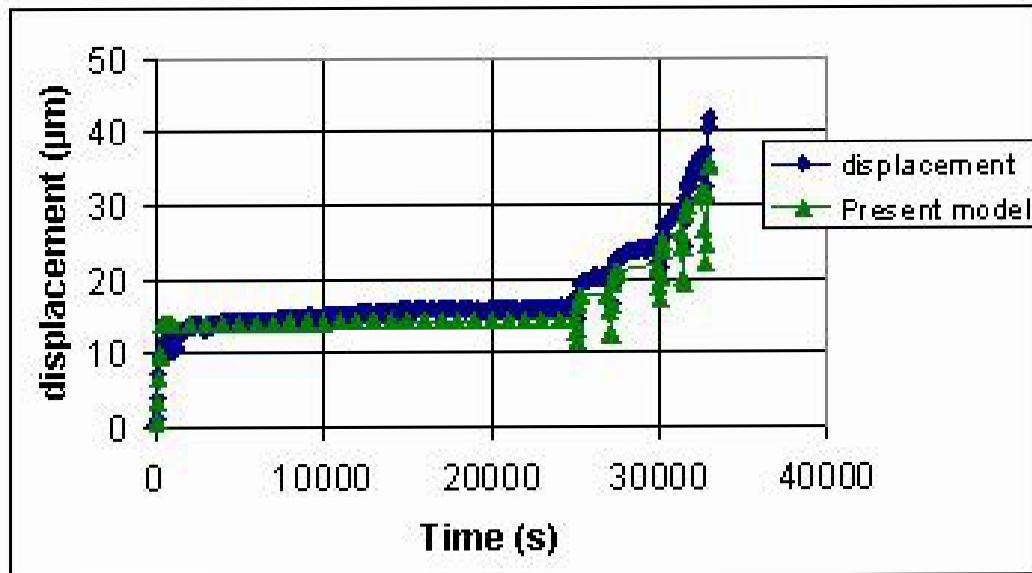


Figure 1.3: Comparison between experimental and theoretical displacement during a bending test

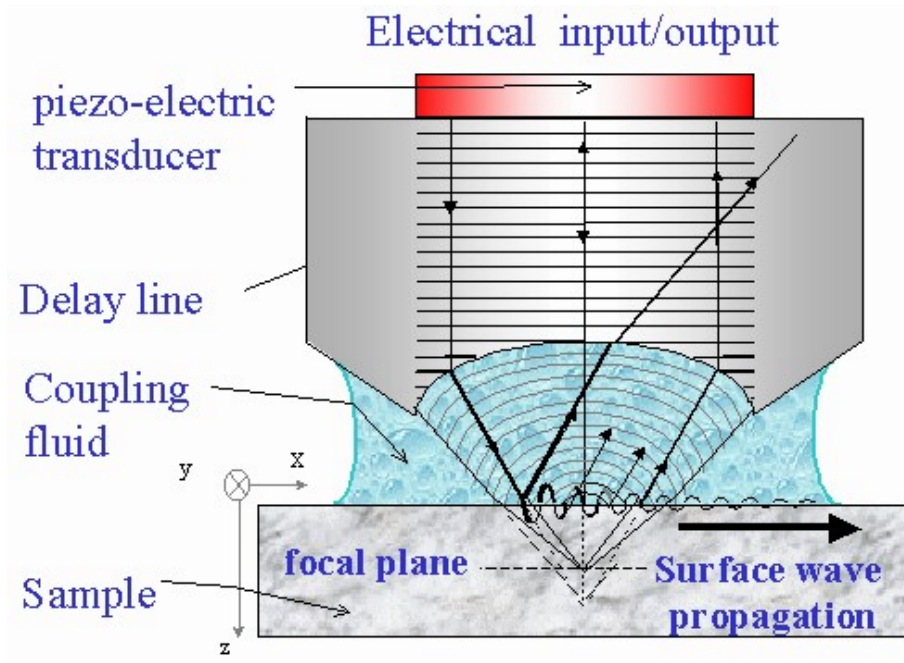


Figure 2.1 – Acquisition of the acoustic signature

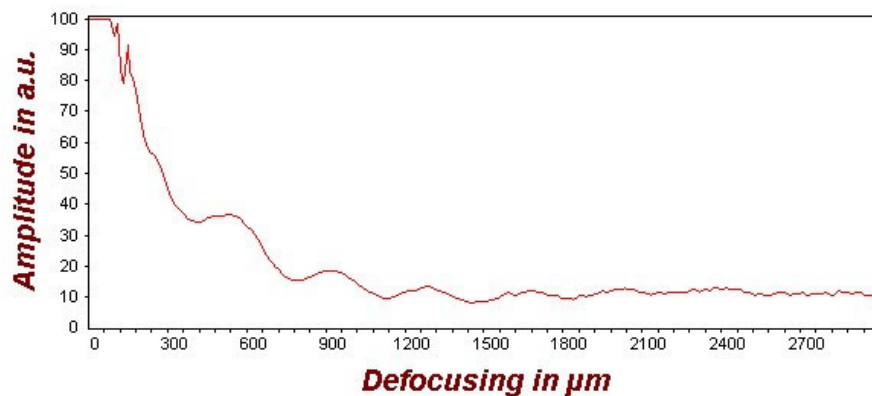


Figure 2.2 – Typical signature on UO_2

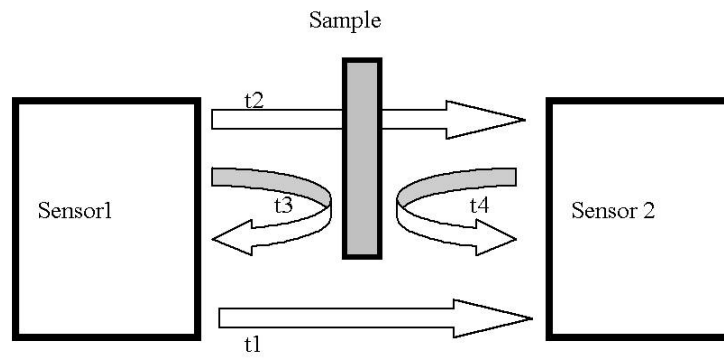


Figure 2.3 – Principles of echography

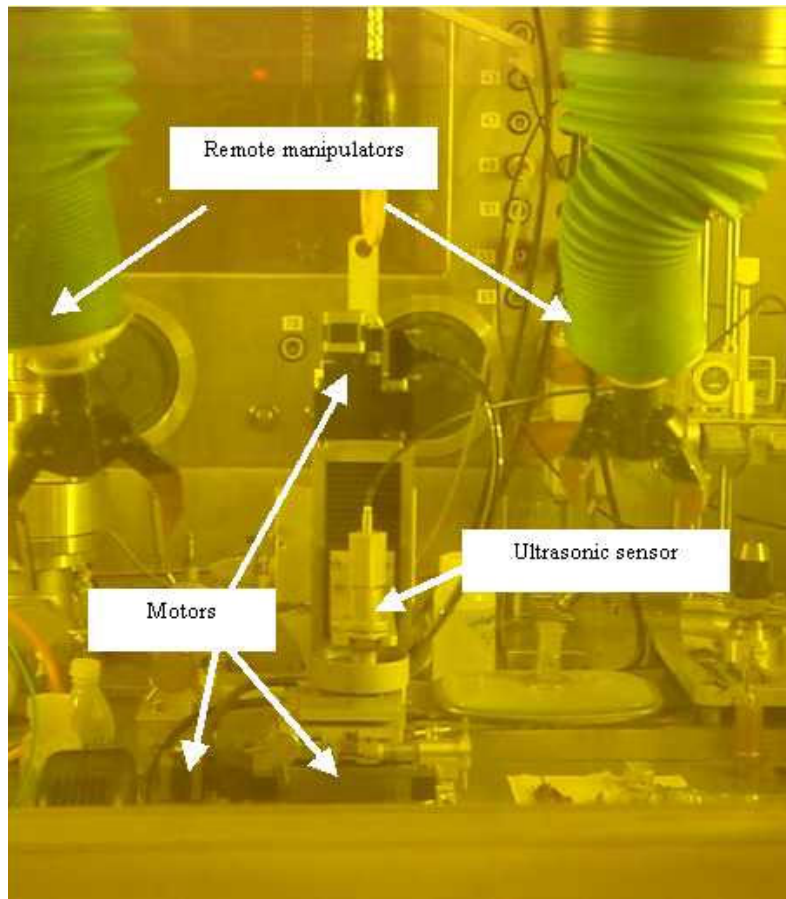


Figure 2.4 – Experimental device introduced in hot cell

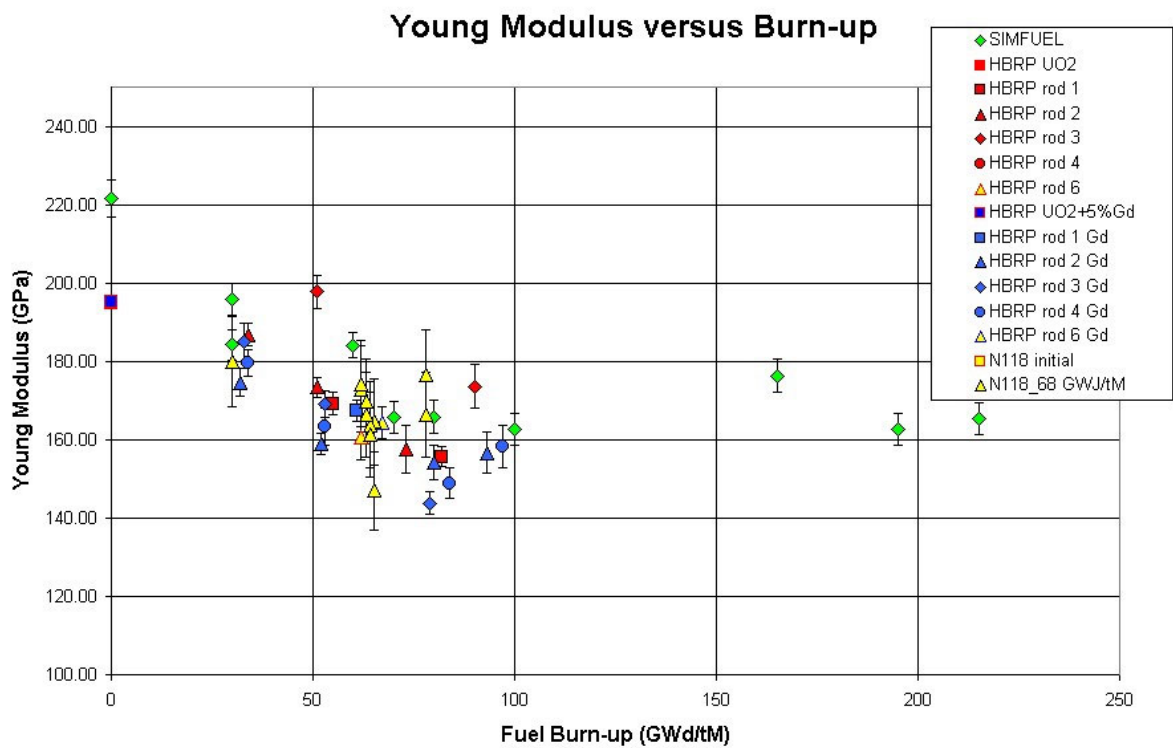


Figure 2.5 – Young modulus versus burn-up - Measurements conducted on the HBRP samples, the N118 fuel rod samples and simulated fuel samples

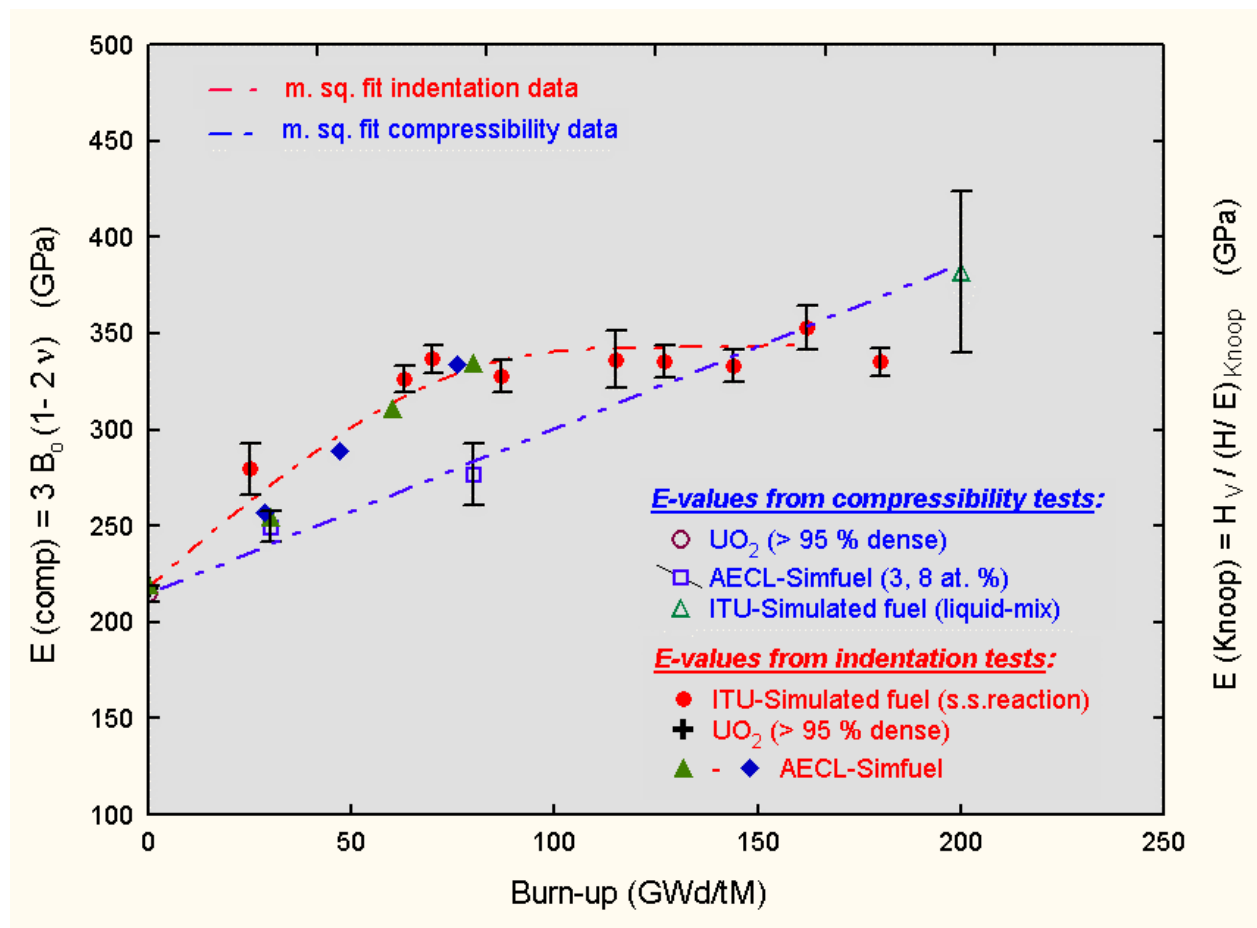
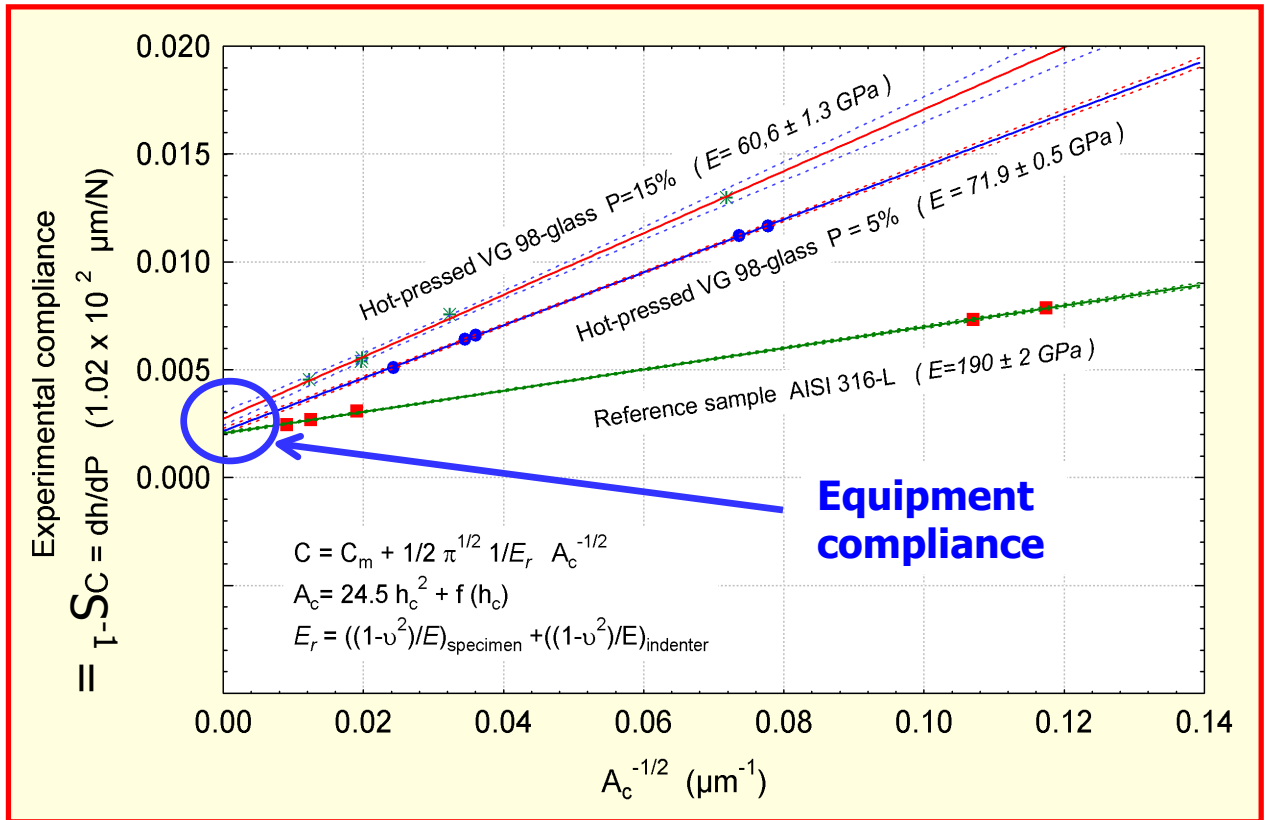


Figure 3.1. – Comparison of Young's modulus values of pure and doped UO_2 from compressibility and Knoop indentation tests [40]



E_{316-L} measured: $190 \pm 2 \text{ GPa}$
 E_{316-L} literature : $192-198 \text{ GPa}$

Fig. 4.1. Examples of Young's modulus determination by instrumented indentation on SS 316 L and porous glass samples []

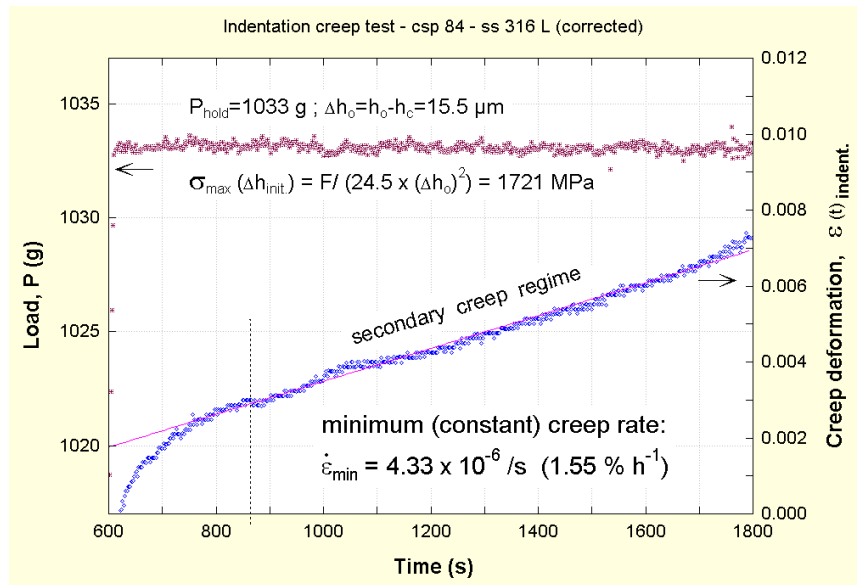
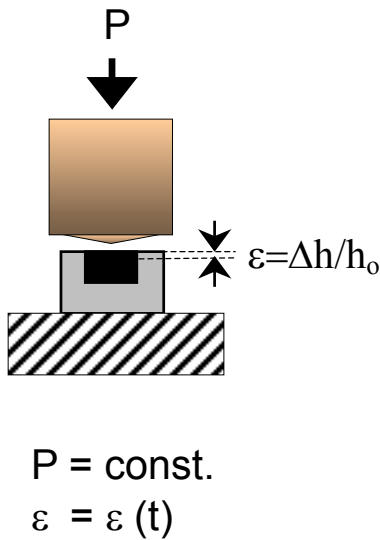


Fig. 4.2 Example of room-temperature indentation creep test on SS 316 L

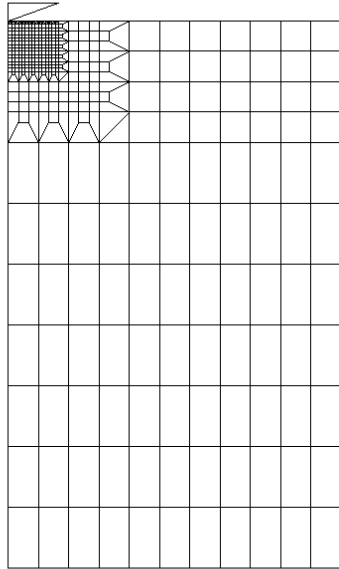


Figure 4.3 – Two-dimensional mesh for indentation test's mechanical simulations.

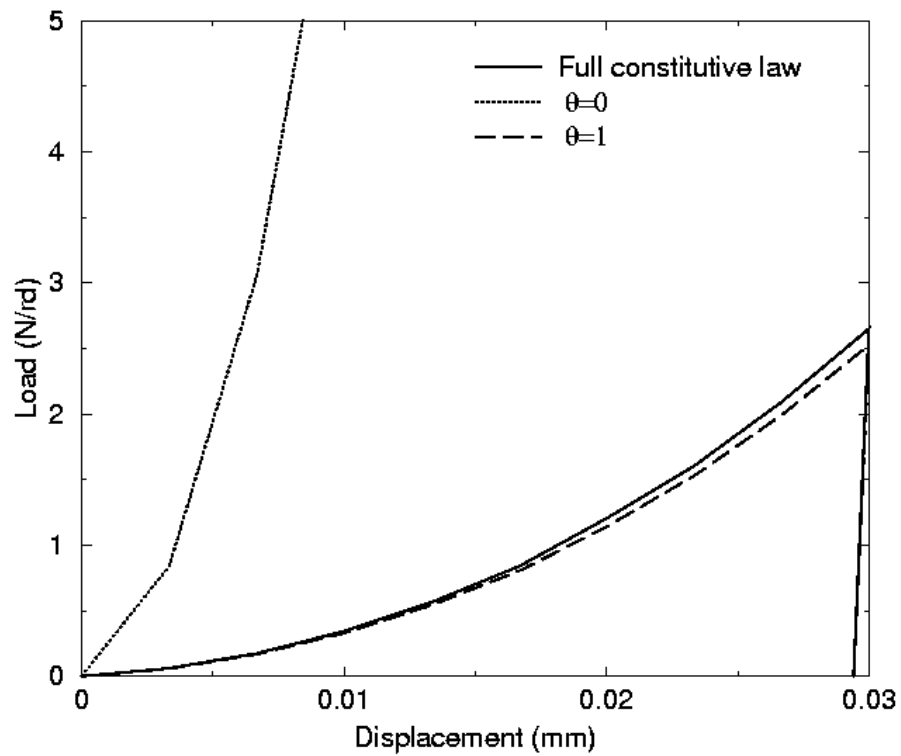


Figure 4.4 – Load displacement curve during indentation of a 100 % dense UO_2 sample (grain size ≈ 6 microns) at 1200°C (constant 30 microns/h displacement rate). Results derived with the constitutive law presented in section 1 (continuous line) are compared to the ones derived with two alternative versions of this model corresponding to a theta-function equal to 0 (dotted line) or 1 (long dashed).

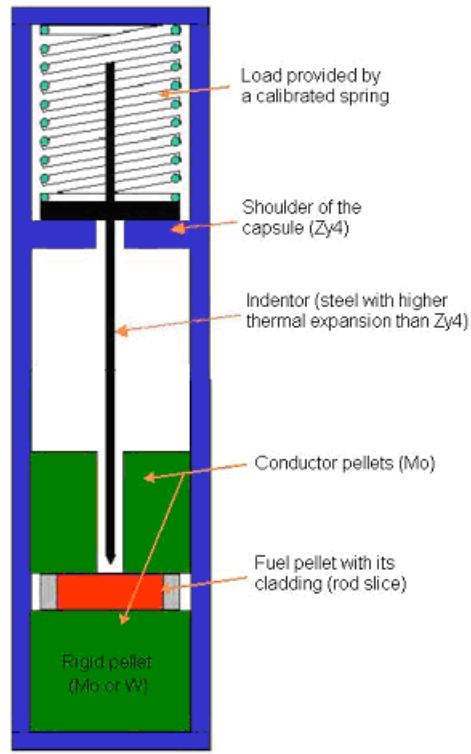


Figure 5.1 – In Pile indenter device

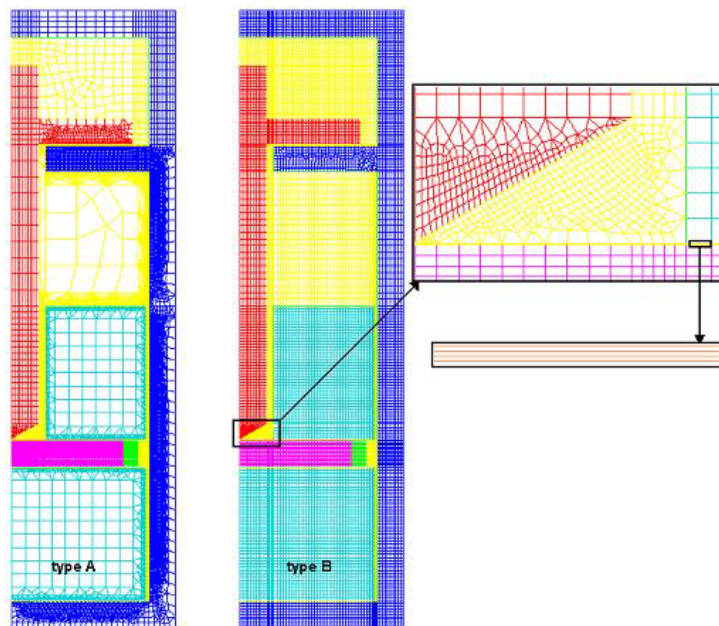


Figure 5.2 - Two-dimensional meshes of the device..

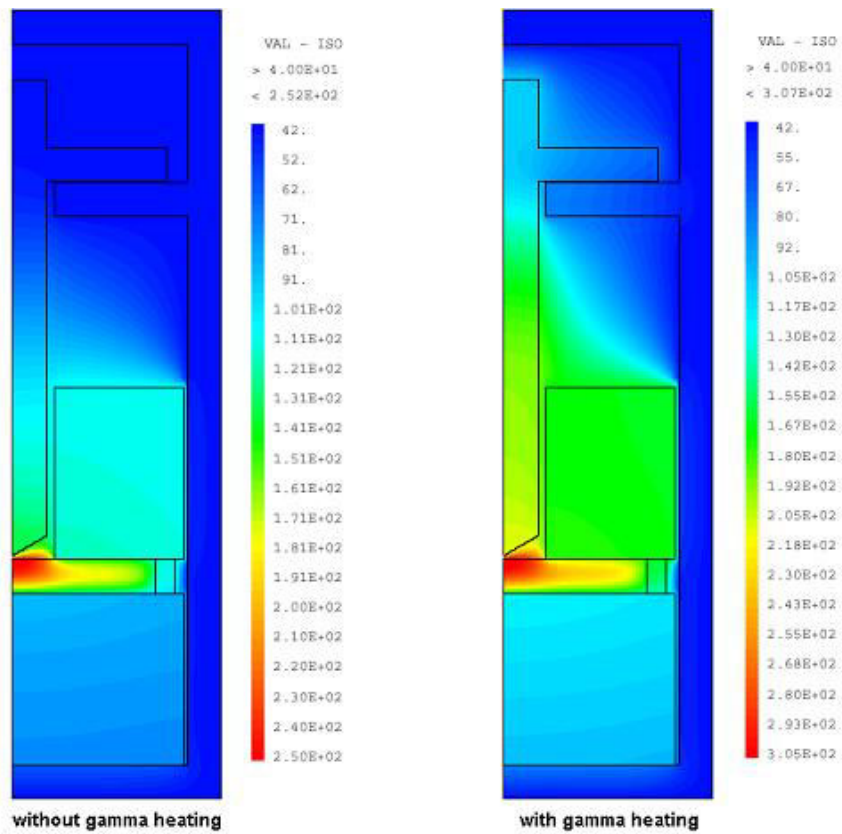


Figure 5.3 - Temperature distributions for a power of 50 kW/m without gamma-heating (left) and with 10 W/g gamma- heating (right)

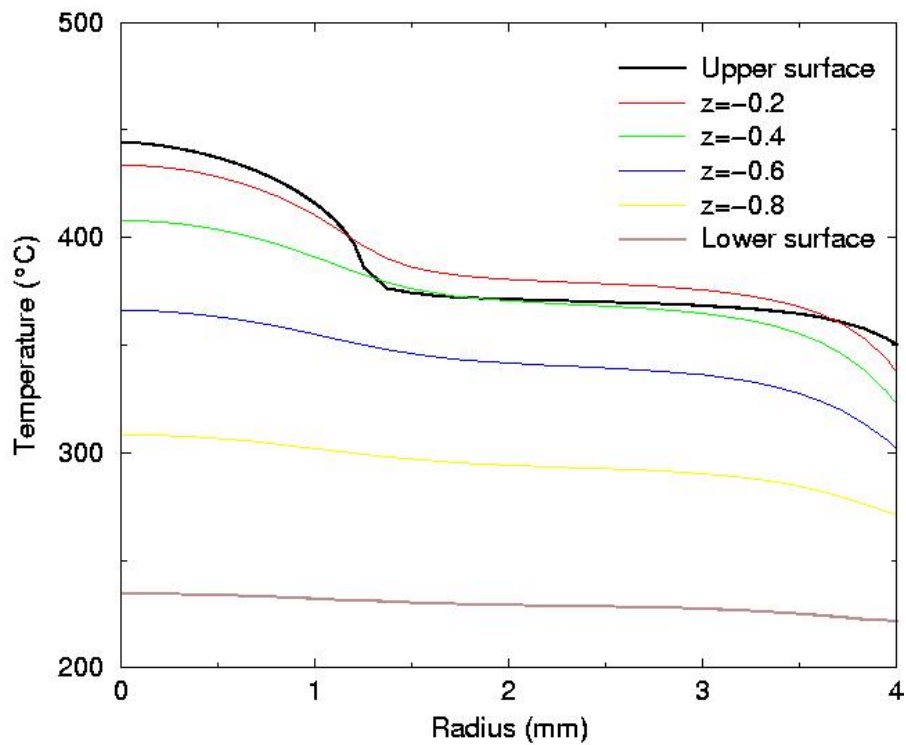


Figure 5.4 - Radial temperature distribution for different axial locations in the fuel wafer (LHR=500W/cm, proposed design concept (Argon filling gas, Indenter's length = 100 mm)).

Fuelling A Clean Future
9th International CNS Conference on CANDU Fuel
Belleville, Ontario, Canada
September 18-21, 2005

*Evolution of the Nuclear Fuel Mechanical properties at
high Burn-up
An Extensive European Experimental Program
Daniel Baron, Renaud Masson, et al.*